VOL 97 No 2
June 2006

SAIEE Africa Research Journal

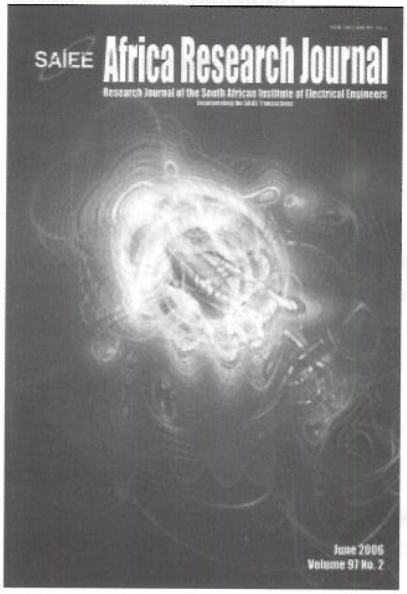

SAIEE AFRICA RESEARCH JOURNAL

(SAIEE FOUNDED JUNE 1909 INCORPORATED DECEMBER 1909)
AN OFFICIAL JOURNAL OF THE INSTITUTE
ISSN 1991-1696

Published by
SAIEE Publications (Pty) Ltd, PO Box 751253, Gardenview, 2047,
Tel. (27-11) 487-3003, Fax. (27-11) 487-3002,
E-mail: SAIEEPublications@saiee.org.za

ARTICLES SUBMITTED TO THE SAIEE AFRICA RESEARCH JOURNAL ARE FULLY PEER REVIEWED PRIOR TO ACCEPTANCE FOR PUBLICATION

The following organizations have listed SAIEE Africa Research Journal for abstraction purposes:
INSPEC (The Institution of Electrical Engineers, London); "The Engineering Index" (Engineering Information Inc.)

PROPAGATION MEASUREMENTS AND MULTIPATH CHANNEL MODELLING FOR LINE-OF-SIGHT LINKS AT 19.5 GHZ

K. Naicker* and S. H. Mneney**

* *Defence, Peace, Safety and Security (DPSS), Council for Scientific and Industrial Research (CSIR), PO Box 395, Pretoria, 0001, South Africa*
** *Centre for Radio Access Technologies, School of Electrical, Electronic and Computer Engineering, University of KwaZulu-Natal, Durban, 4041, South Africa*

Abstract: The need for greater bandwidth and higher data rates will inevitably lead to the usage of the upper portion of the k-band in terrestrial communication systems. The frequency band from 18 GHz to 20 GHz has been identified as a suitable candidate for short-haul line-of sight links. As a consequence, a 6.73 km terrestrial LOS link centered at 19.5 GHz has recently been established between the Howard College and Westville campuses of the University of KwaZulu-Natal (UKZN), with the primary objective to investigate the effect of rain attenuation over the link. Multipath propagation and the resultant frequency selective fading is another major problem afflicting such LOS links. In order to evaluate the effect of multipath propagation over the link statistical models of the channel transfer functions are required. In this paper the research into the simulation and statistical modeling of the multipath propagation for the above-mentioned LOS link will be discussed.

Key words: multipath propagation modelling, multipath fading, channel transfer function modelling, terrestrial line-of-sight links, path profiling, propagation measurements.

1. INTRODUCTION

During the planning of terrestrial line-of-sight (LOS) systems, quantitative data relating to the fade margin, fade duration as well as the flat and frequency selective characteristics of the channel are required. In order to examine the feasibility of an alternative broadband carrier, the necessary propagation measurements and channel models are required. This paper will discuss the research into the modeling and measurement of the specified terrestrial LOS link operating at 19.5 GHz.

The research aims to characterise the performance of the link by evaluating the effects of multipath propagation under various meteorological conditions. A LOS link was established between the Howard College and Westville campuses of UKZN and passes over both hilly and suburban terrain. The channel response will be examined over a 200 MHz bandwidth centered at 19.5 GHz.

In the mid 1970s the Wave Propagation Standards Committee of the IEEE sponsored several mini-reviews into the absorption of radio waves in the atmosphere. The work by [1] focused on the effect of oxygen and water vapour in the atmosphere and [2] on rain attenuation. From these mini-reviews, the following conclusions were arrived at,

1) Radio frequencies above 15 GHz were attractive because of their limited use at the time and since they could provide larger bandwidths.
2) The presence of water vapour and oxygen in the lower atmosphere resulted in peak absorption attenuations near 22 GHz and 60 GHz, respectively.
3) There were three regions of lesser attenuation around 35 GHz, 90 GHz and 225 GHz.
4) However, in near-earth conditions the attenuation at the 90 GHz and 225 GHz regions was even greater than that for the maximum loss from the 22 GHz vapour line. Hence these frequencies are more suitable for satellite-earth communication systems. If rain losses were considered, the 35 GHz region was even more opaque than the 22 GHz region.

This motivates the idea of using the upper portion of the k-band for short-haul point-to-point terrestrial communication links. For the majority of time, such LOS microwave links will operate essentially error free. The transmission medium, which is the lower part of the atmosphere, is usually non-dispersive making the transmission of high-speed digital data highly reliable. However, being a natural medium, anomalous behaviour in the troposphere can still occur for some fraction of time and this can result in multipath propagation. The consequence is multipath fading consisting of both flat and frequency-selective components and this can cause severe degradations in system performance.

The flat fading component produces a time-variant, attenuation that is uniform across the entire channel bandwidth. Rain along the propagation path is one example of a source of flat fading.

The frequency-selective fading component, on the other hand, results in non-uniform attenuation in the form of slopes or notches within the channel bandwidth. Such fading often occurs during periods of time when there is an irregular variation in the refractive index of the atmosphere.

In order to combat such undesirable channel phenomena, system designers need realistic and readily useable models of the multipath channel responses at their disposal. To achieve this, long term experiments need to be implemented. Hence, the above-mentioned LOS link was recently established. However, such experiments are few and far between. One approach in overcoming the scarcity of experimental measurements is to use computer generated transfer functions and this will be the focus of this paper.

This paper is organized as follows. In Section 2, a brief review of the different channel transfer models are given. Section 3 provides a description of the equipment followed by path profiling in Section 4. Section 5 describes the modelling and simulation of channel transfer functions. The results for the fixed delay two-ray model and complex polynomial expansion are discussed in Sections 6 and 7, respectively. Concluding remarks are given in Section 8.

2. PROPAGATION MEASUREMENTS AND MODELING

Propagation studies for line-of-sight links date back to when FM systems were first introduced in the early 1950's. Although substantial research was devoted in this field, the need for comprehensive models only emerged with the advent of digital radios in the 1970's.

Since then several detailed models [3]-[6] have been developed for the common carrier bands used in digital radio systems, namely, 4, 6 and 11 GHz. Each provides an alternative approach in the statistical modelling of the multipath effects on line-of-sight links.

In [3] a measurement-derived three-path model was established, given by the following channel transfer function,

$$H(.) = a\left[1 - be^{\pm j(. - .0)\tau}\right] \quad (1)$$

where, τ is the delay difference and $.0$ is the notch frequency of fade minimum. It is assumed that there is a negligible time delay between the direct LOS ray and the 2nd refracted ray. Subsequently a represents the vector sum of the first two paths and ab is the magnitude of the third path. In [3], the model was further simplified by assuming a fixed delay, τ, given by,

$$\tau = \frac{1}{6B} \quad (2)$$

where, B, is the bandwidth under consideration. This results in a fixed delay two-ray model.

A similar approach was adopted in [5], except instead of assuming a fixed delay, the four parameters of (1) were reduced to three by imposing $a = 1$, thus resulting in a normalized two-ray model.

An alternative approach was shown in [4], where the channel transfer function was modelled by the complex polynomial representation given by:

$$H_c(.) = A_0 + \sum_{n=1}^{N}(A_n + jB_n)(j.)^n \quad (3)$$

where, $. = . - .c$, is the frequency measured relative to the centre frequency, $.c$. It was further shown in [4] that a good representation of the same measurement data used in [3] is possible with a first order polynomial.

In [5] it was demonstrated that the parameters of the normalized two-ray model, b, $.0$ and τ can be obtained from a transformation of the parameters of a first order complex polynomial given by (3).

The complex polynomial model and the fixed delay two-ray model will be examined in this paper and will be discussed further in Sections 6 and 7.

3. DESCRIPTION OF EQUIPMENT

3.1 Transmitter and Receiver Station

A system for monitoring the channel response under various meteorological conditions was installed on the 6.73 km overland path separating the two campuses of the UKZN. A block diagram of the system is provided in Figure 1.

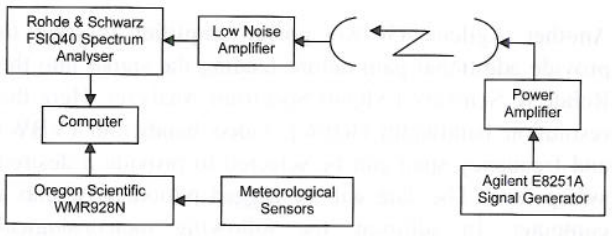

Figure 1: Block diagram of the monitoring system

The transmitter station was setup on the roof of the Science Building at the Westville campus and the corresponding receiver station was established on the roof of the Electrical Engineering Building located within the Howard College campus. This provides sufficient

clearance for the LOS link, which passes over both hilly and suburban terrain.

3.2 Antennae and Cabling

Valuline® WR42/R220 parabolic antennae of diameter 0.6 m are used at both the receiving and transmitting stations. The multiband antennae can operate within the 17.7 -19.7 GHz and 21.2 -23.6 GHz bands and provide a gain of 38.6 dBi and a 3 dB beamwidth of 1.9 degrees at 19.5 GHz. The cabling consists of FSJ1-50A superflexible coaxial cables of length 6 m at the transmitter and 5.5 m at the receiver.

3.3 Transmitter

The Agilent E8251A signal generator is used to provide the source signal. It can supply an output power of –135 dBm to +13 dBm and can operate up to 20 GHz. It can also provide both AM and FM modulation schemes. To provide a signal from 10-100 mW to the parabolic antenna, a preamplifier is used. The Agilent 83018A power amplifier is used and it can operate from 2 GHz to 26.5 GHz and provide a gain of 27 dB. The following modes of operation are thus possible:

1) Fixed frequency, unmodulated continuous wave (CW),
2) Narrowband Sweep (50 MHz),
3) Broadband Sweep (200 MHz),
4) AM Modulation
5) FM Modulation.

To date, CW (fixed frequency) signals have been transmitted and recorded for calibration and setup, as well as to examine the effects of rain on the signal strength. A few narrowband sweeps and broadband sweeps have been taken and once sufficient datasets have been recorded the channels transfer function will be modelled as described in Section 5. Modulated signals can be used later to determine the delay spread.

3.4 Receiver

Another Agilent 83018A power amplifier is used to provide additional gain before feeding the signal into the Rohde & Schwarz FSIQ40 Spectrum Analyzer. Here the resolution bandwidth (RBW), video bandwidth (VBW) and frequency span can be selected to provide a desired sweep time. The data will be logged periodically onto a computer. In addition, the following meteorological conditions are also logged using the Oregon Scientific WMR928N Wireless professional weather station:

1) Outdoor Temperature (-20°C to 60°C)
2) Rainfall Rate (0 to 9999 mm/h)
3) Relative Outdoor Humidity (2% to 98%)
4) Outdoor Dew Point Temperature (-10°C to 60°C)
5) Outdoor Pressure (795 to 1050 mbar)
6) Wind Speed (0 to 56 m/s) and
7) Wind Direction (0° to 359°)

4. PATH PROFILING

4.1 The Path Profile

The measurements will initially be taken over a period of one year examining the effects of the varying meteorological conditions. The link passes over both hilly (near Westville) and suburban (near Cato Manor) terrain. An aerial map of the link is provided in Fig. 2.

Due to the high directive gain of the parabolic antennas used at each of LOS stations, accurate pointing is required. The azimuth details are obtained using the latitude and longitude coordinates of each station (see Figure 2). The distance between the two base stations is 6.73 km.

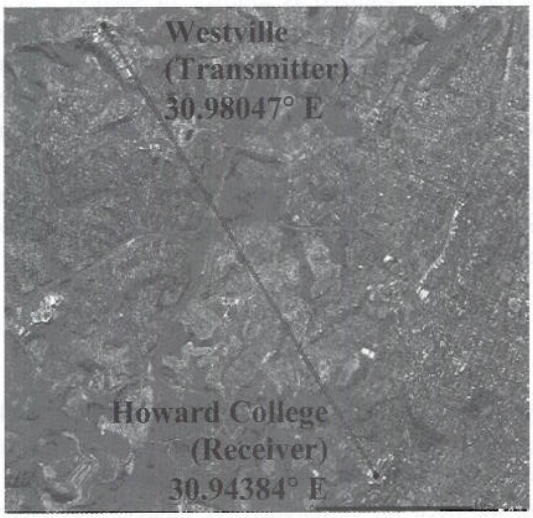

Figure 2: An aerial photograph of the LOS terrestrial link

The azimuth required at the Westville transmitter station is 328.34° and the azimuth at the Howard College receiver station is 148.32°. These azimuth angles are measured clockwise from the reference of the magnetic south. The various terrestrial link parameters such as altitude and antennae heights are given in Table 1.

The path profile is shown in Figure 3 and contains an adjustment to account for the vegetation and buildings along the line-of-sight.

4.2 Path Clearance

According to ITU recommendations [9], diffraction fading can be reduced if the antennae heights are sufficiently high so that even in the worst case of refraction, there is still sufficient clearance above any path obstacles. Fresnel ellipsoids can be used to estimate the diffraction and reflections along the path. The radius of the first Fresnel ellipsoid is given by:

$$F_1 = 17.3\sqrt{d_1 d_2 / fd} \quad (4)$$

where F_1 denotes the radius of the first Fresnel ellipsoid (m), f is the frequency (GHz), d is the path length (km) and d_1 and d_2 the distance from either station (km). The path clearance from the first Fresnel ellipsoid and the LOS path are also shown in Figure 3. A k-factor or effective radius factor smaller than one can be used to examine the clearance for the worst case of ray bending.

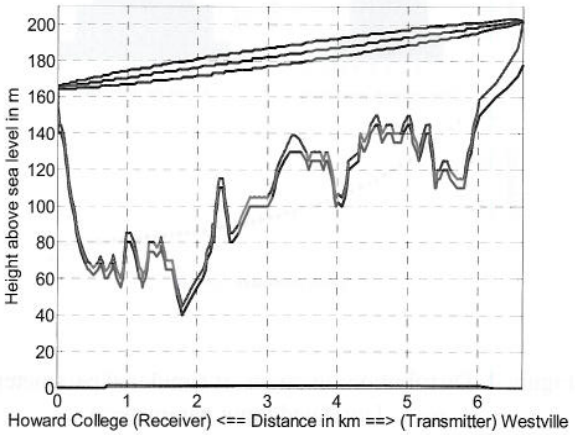

Figure 3: The path profile for the 6.73 km LOS link between the Howard College and Westville campuses

TABLE 1
TERRESTRIAL LINK PARAMETERS

Parameter	Description
Path length	6.73 km
Height of transmitting antenna above the ground	24 m
Altitude of transmitter station	178 m
Height of receiving antenna above the ground	20 m
Altitude of receive station	145 m
Carrier frequency	19.5 GHz
Bandwidth under investigation	200 MHz
Transmitter power	10-100 mW
Transmitting/receiver antenna gain	38.6 dBi
Transmitting/receiver antenna beamwidth	1.9 degrees
Free space loss	135 dB
Total cabling and connector losses	22 dB
Clear air attenuation	1 dB
Receiver bandwidth	100 kHz -1 GHz

5. MODELING AND SIMULATION OF THE MULTIPATH CHANNEL TRANSFER FUNCTION

The fundamental aim of this research is to model the effects of the atmosphere on terrestrial line-of-sight links operating in the upper portion of the k-band. The key questions that need to be answered are:

1. Do existing multipath models [3] and [4] still hold for the frequency range under examination?
2. How do the multipath model parameters vary for these higher frequency ranges?
3. Are the models extendable to larger bandwidths?
4. How applicable are these models to other LOS links?

Computer simulations can provide a vital tool in answering these questions and in the modelling of multipath channels. Once simulated channel transfer functions have been generated, they can be statistically analysed and mathematically modelled as discussed in Section 2. The statistical variability of the model parameters can then be examined for various simulated channel transfer functions.

In [7] the statistical behaviour of multipath channels was examined and a method of simulating channel transfer functions was then developed. The channel transfer functions were generated by causing several simulated rays to interfere with one another. These simulated rays were dependent on several input parameters, namely, the number of interfering rays, N, the ray amplitudes, a_k, ray delays, τ_k, and the ray phases, ϕ_k. In [7], three different approaches of generating the transfer functions were examined. In each case, the channel transfer functions were then statistically analyzed and mathematically modelled using the normalized two-ray model. The results were then compared to measured results from the PACEM2 experiment, namely 11.5 GHz.

A simulation approach based on [7] was adopted for the 19.5 GHz LOS link. The simulated transfer functions were then modelled using the two approaches mentioned in Section 2, namely the fixed delay two-ray model and complex polynomial expansion model. The statistical parameters of each model were then examined, as in [10] and [11], the results of which are discussed in Sections 6 and 7.

5.1 The Simulation Input Parameters

The simulation procedure discussed in [7] consists of allowing N rays to interfere with one another, resulting in the transfer function $\tilde{H}$, given by,

$$\tilde{H}(f) = \sum_{k=1}^{N} a_k e^{-j(2\pi f \tau_k - \phi_k)} \quad (5)$$

where N is the number of rays, a_k, τ_k and ϕ_k is the amplitude, delay and phase shift of the k^{th} ray, respectively.

The next step is to determine the reduced transfer function, which is the ratio of the actual transfer function to a non fade or flat transfer function. This flat reference level is designated as A_0, which is given by,

$$A_0 = \frac{\langle N \rangle \langle a_k \rangle}{\sqrt{2}} \quad (6)$$

where, $\langle N \rangle$ is the mean number of rays and $\langle a_k \rangle$ denotes mean value of the amplitudes.

The values for the simulated parameters were then generated according to the distribution functions suggested by [7]. In the first case the input parameters were assumed to be unrelated. The second case considered dependence on the ray angle-of-arrival (AOA) and in the third case the interfering rays were divided into three distinct groups, namely the atmospheric refracted group, the direct group and the ground-reflected group.

For each case, these respective distribution functions were then used to generate the ray number, N, and thereafter N values for the amplitude, delay and phases of the rays. These input parameters were then used to generate the transfer function sampled at 1 MHz steps over the frequency range from 19.4 GHz to 19.6 GHz. The transfer function was then transformed, with respect to the centre frequency of 19.5 GHz, and normalised using the reference level, A_0. This process was repeated until 100 000 reduced transfer functions were obtained for each case.

When actual channel measurements are taken, the channel will be swept at 1 MHz intervals over the 200 MHZ bandwidth. Each power measurement will be recorded in dB and referenced to the average power level of that frequency at mid-day. The resultant data from each sweep will thus give a reduced transfer function of the channel.

Next, an occurrence criterion is applied to the reduced transfer functions, so as to retain only those transfer functions whose attenuation at any frequency in the bandwidth considered is greater than some threshold, T. An attenuation threshold of $T = 5$ dB and $T = 10$ dB was used. The transfer functions meeting these criterions are then modelled using the fixed delay two-ray model and then the complex polynomial expansion.

5.2 Case 1: Unrelated Input Parameters

In the first approach, it is assumed that the amplitudes, delays and phases are mutually independent and unrelated to the ray number, N. As discussed in [7], N, follows a modified binomial distribution and range from 2 to 10 rays. The ray amplitudes, a_k, are given by,

$$a_k = (1/\pi)\arccos(1-2x) \quad (7)$$

where, x is a [0,1] uniformly distributed random variable. The reference level, A_0, was subsequently calculated to be equal to 1.777. The ray phase shifts, ϕ_k, follow a uniform distribution over the range $[0, 2\pi]$. The ray delays, τ_k, are given by:

$$\tau_k = -\gamma \ln(x) \quad (8)$$

where $\gamma = 0.5ns$, as in [7]. The distribution functions for the simulated parameters are shown in Figure 4.

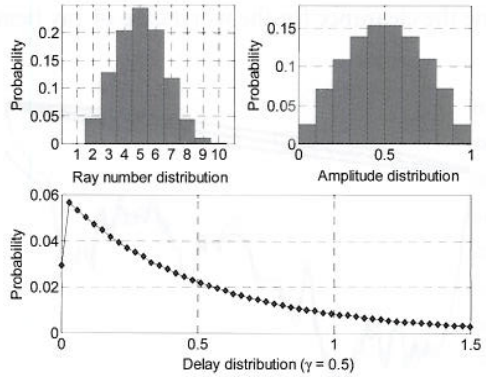

Figure 4: Distribution functions of simulated parameters (Case 1: Unrelated input parameters)

5.2 Case 2: Dependence on AOA

In this approach, the concept of ray AOA is introduced along with the dependence of the ray amplitudes and delays on this parameter. The ray phase shifts, ϕ_k, and N, are still assumed to be independent and are still determined as discussed in the first case.

The AOA, α, is given by,

$$\alpha = \frac{2\alpha_{max}}{\pi}\arcsin(2x-1) \quad (9)$$

where α and α_{max} are in radians and x is a [0,1] uniformly distributed random variable. Typical values for α_{max} can range from 0.1° to 1°. In this case $\alpha_{max} = 0.5°$ is assumed.

The ray amplitudes, a_k, are then given by,

$$a_k = 10^{-20|\alpha|} \quad (10)$$

The reference level, A_0, was calculated to be equal to 3.085 and $\langle a_k \rangle$ is found to be 0.868.

To generate the ray delay it is assumed that the simulated ray is reflected at a point in the middle of the hop length, D, and that the reflected ray forms an angle, α, with respect to the direct ray.

The ray delays, τ_k, are now subsequently given by,

$$\tau_k = \frac{D}{c}\frac{\alpha^2}{2} \tag{11}$$

where c is the speed of light and $D = 6.73$ km. The distribution functions for the above mentioned simulated parameters are shown in Figure 5.

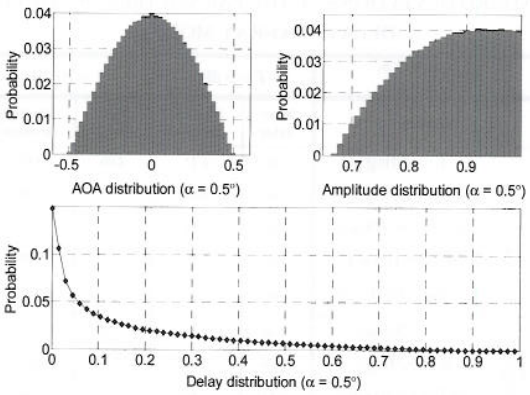

Figure 5: Distribution functions of simulated parameters (Case 2: Dependence on AOA)

5.3 Case 3: Ray Groups

In the last approach, the interfering rays are divided into the three categories as discussed previously. The distribution functions are modified for each group.

For the atmospheric refracted group N, ranges from 0 to 4 rays according to a binomial distribution. The AOA, α, is given by a half-sine distribution, as discussed in the second case, with $\alpha_{\max} = 0.2°$ and an offset of 0.15°.

The direct group consists of a single ray hence, $N = 1$ with $\alpha = 0°$. The ground-reflected group comprises of 2 to 5 rays, generated according to a modified binomial distribution as discussed in the first case. The AOA, α, is again given by a half-sine distribution, as discussed in the second case, with $\alpha_{\max} = 0.6°$ and an offset of -0.2°. For all groups the ray delays and ray phase shifts are given as discussed in the second case.

Thus in the third case, the total number of rays ranges from 3 and 10 rays. The reference level, A_0, was subsequently calculated to be equal to 3.614. The distribution functions for the above mentioned simulated parameters are shown in Figure 6.

For each of the simulation cases, 100 000 transfer functions were generated. Table 2 contains the number of transfer functions retained after the attenuation threshold criteria of $T = 5$ dB and $T = 10$ dB were applied. These transfer functions, which were then, modelled using the fixed delay two-ray model in Section 6 and the complex polynomial expansion in Section 7.

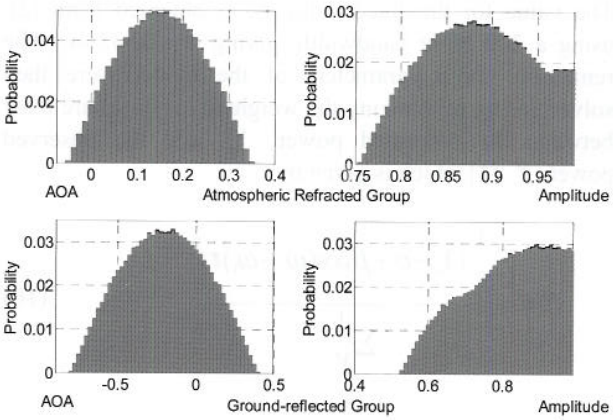

Figure 6: Distribution functions of simulated parameters (Case 3: Ray Groups)

TABLE 2
NUMBER OF TRANSAFER FUCTIONS RETAINED AFTER ATTENUATION THRESHOLD CRITERIA ARE APPLIED

ATTENUATION THRESHOLD	$T = 5$ dB	$T = 10$ dB
CASE 1 : UNRELATED	60958	29938
CASE 2 : AOA DEPENDENCE	58501	25622
CASE 3 : RAY GROUPS	65294	31049

6. THE FIXED DELAY TWO-RAY MODEL

The fixed delay two-ray model was introduced by [3] to model a 26.4 MHz bandwidth at 6 GHz. The dataset included 25000 scans of the channel bandwidth, with each scan recording the power measurements at 24 frequencies separated 1.1 MHz apart. This model will now be applied to the two simulated datasets for $T = 5$ dB and $T = 10$ dB.

$$Y_n = Y(\omega_n) \text{ for } n = 1,2,\cdots,200 \tag{12}$$

$$\omega_n = 2\pi n\left(1\times10^6\right) \text{ for } n = 1,2,\cdots,200 \tag{13}$$

A model for the voltage transfer function, $H(\omega)$, given by (1) is then obtained by estimating Y_n with,

$$\hat{Y}_n = \left|H(\omega_n)\right|^2 = \alpha - \beta\cos(\omega_n - \omega_0)\tau \tag{14}$$

where α and β can be related to a and b of (1) as follows,

$$\alpha = a^2\left(1+b^2\right)$$
$$\beta = 2a^2b \tag{15}$$

The value for the fixed delay, τ, is obtained from (2), using a 200 MHz bandwidth, giving $\tau = 0.833\ ns$. The remaining three parameters of the model were then solved for by minimizing the weighted mean-square error between the estimated power, Y_n, and the observed power, $\hat{Y}_n$ [3] which is given by:

$$E = \frac{\sum \frac{1}{Y_n}\left(Y_n - \alpha + \beta\cos(\omega_n - \omega_0)\tau\right)^2}{\sum \frac{1}{Y_n}} \qquad (16)$$

with the constraint, $\alpha > \beta$. If $\alpha < \beta$ then the solution yields complex-values for a and b. Real values can still be acquired for these transfer functions by moving ω_0 away from the initial optimum value and re-optimizing. The datasets for each simulation case were modelled as discussed with the constraint, $\alpha > \beta$. If $\alpha < \beta$ then the solution yields complex-values for a and b. Real values can still be acquired for these transfer functions by moving ω_0 away from the initial optimum value and re-optimizing. The datasets for each simulation case were modelled as discussed above. Table 3 contains the percentage of transfer functions that result in complex-valued solutions. These transfer functions have either little shape or a steep slope across the bandwidth.

TABLE 3
PERCENTAGE OF DATASET WITH COMPLEX-VALUED SOLUTIONS FOR ALL THREE CASES AND ANTENNUATION THRESHOLD

ATTENUATION THRESHOLD	$T = 5$ dB	$T = 10$ dB
CASE 1 : UNRELATED	16.7 %	14.2 %
CASE 2 : AOA DEPENDENCE	0.3 %	0.7 %
CASE 3 : RAY GROUPS	13.4 %	13.1 %

Parameters a and b relate to the shape and scale of the multipath fade. These parameters are expressed logarithmically, with the mean and standard deviation given in Table 4.

The parameter A is fade level or loss term and B relates to the relative notch depth. The parameter Γ is a useful indication of the shape of the gain curve given that $\beta/(\beta-\alpha)$ is effectively the ratio of the radius of curvature to the level of the notch. It is apparent that the choice of threshold has a greater effect on the mean values as opposed to the standard deviation. Also the parameter *BETA* seems to be less affected. Histograms for these parameters are given in Figure 7.

The shape of the distribution functions are smooth and may be expressed as conventional statistical distributions, such as normal and gamma laws. The choice of threshold clearly has a windowing effect on the distribution functions.

The scatter diagrams of the parameters *ALPHA* and *BETA* for case 1 (unrelated parameters) are given in Figure 8. The upper curve limit is the straight line corresponding to the constraint $\alpha > \beta$. The lower curved limit is effect attenuation threshold.

TABLE 4
EFFECT OF THRESHOLD ON THE MEAN VALUES AND STANDARD DEVIATIONS OF THE PARAMETERS OF THE FIXED DELAY TWO-RAY MODEL

ATTENUATION THRESHOLD		$T = 5$ dB		$T = 10$ dB	
	Parameter	Mean Value	Standard Deviation	Mean Value	Standard Deviation
CASE 1 : UNRELATED	$A = -20\log a$	6.98	4.11	8.48	4.69
	$B = -20\log b$	9.93	8.41	6.75	6.96
	$ALPHA = 10\log\alpha$	-6.06	4.38	-7.16	5.20
	$BETA = 10\log\beta$	-8.93	6.46	-8.85	6.96
	$\Gamma = \log[\beta/(\beta-\alpha)]$	1.08	2.31	2.11	2.42
CASE 2 : AOA DEPENDENCE	$A = -20\log a$	9.16	3.86	12.42	3.52
	$B = -20\log b$	16.70	9.52	12.64	8.55
	$ALPHA = 10\log\alpha$	-8.83	3.69	-11.85	3.46
	$BETA = 10\log\beta$	-14.50	5.21	-15.73	5.32
	$\Gamma = \log[\beta/(\beta-\alpha)]$	0.62	1.70	0.19	1.82
CASE 3 : RAY GROUPS	$A = -20\log a$	8.59	3.77	11.10	3.68
	$B = -20\log b$	13.15	9.01	9.69	7.78
	$ALPHA = 10\log\alpha$	-8.00	3.72	-10.21	3.87
	$BETA = 10\log\beta$	-12.16	5.60	-12.93	5.86
	$\Gamma = \log[\beta/(\beta-\alpha)]$	0.17	1.99	1.03	2.11

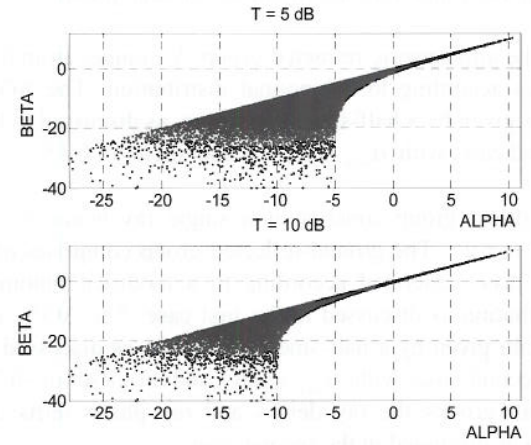

Figure 8: The scatter diagrams of *ALPHA* and *BETA* for case 1 (unrelated input parameters)

Future work will encompass the modelling of measured channel transfer functions from the LOS link, using the above mentioned model. The next step would be to determine what parameter values result in a desired error rate. The outage time for that given error rate can then be determined.

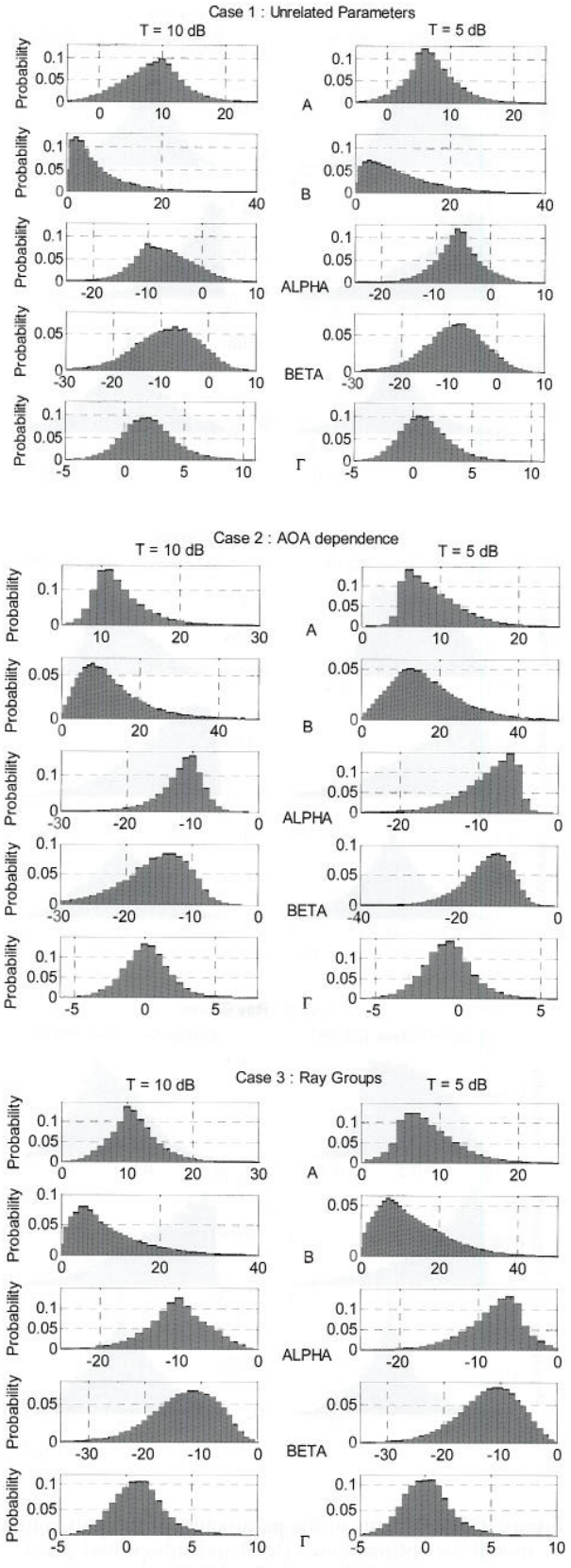

Figure 7: Histograms of the parameters of the fixed two-ray model for attenuation thresholds, $T = 10$ dB (left) and $T = 5$ dB (right)

7. THE COMPLEX POLYNOMIAL EXPANSION METHOD

In this method the power gain transfer functions are fit to a M^{th} order polynomial given by,

$$|H_c(.)|^2 = D_0 + D_1 + \cdots + . \; {}^{M}D_M \tag{17}$$

The coefficients of this polynomial are then used to solve for the parameters of the polynomial expansion, given in (3). It was shown in [5], that a polynomial of order $M = 2$ is sufficient to model observed fading responses. Second order polynomials were thus fit to each of the simulated transfer functions. The coefficients of the polynomial fits, namely, D_0, D_1 and D_2, can then be used to determine . , given by,

$$. = \left(D_2 - D_1^2/4D_0\right) \tag{18}$$

The coefficients of the complex polynomial expansion, can then be solved as follows:

$$\begin{aligned} A_0 &= \sqrt{D_0} \\ B_1 &= D_1/2A \\ A_1 &= \begin{cases} \pm\sqrt{.}; & . = 0 \\ \pm\frac{1}{2}\sqrt{-B_1^2 + |B_1|\sqrt{B_1^2 - 8.}}; & . < 0 \end{cases} \\ A_2 &= \begin{cases} 0; & . = 0 \\ \dfrac{A_1^2}{A_0}\left(1 + \dfrac{A_1^2}{B_1^2}\right); & . < 0 \end{cases} \\ B_2 &= -A_2 B_1 / A_1 \end{aligned} \tag{19}$$

It can be seen that an optimum solution ($A_2 = 0$ and $B_2 = 0$) is possible only if $. = 0$. For the case $. < 0$, a suboptimal solution is obtained by neglecting A_2 and B_2 and using the resulting truncated polynomial. Table 5 contains the percentage of transfer functions that result in suboptimal solutions. The mean and standard deviation for the relevant parameters are given in Table 6

TABLE 5
PERCENTAGE OF DATASET WITH SUBOPTIMAL SOLUTIONS FOR ALL THREE CASES AND ANTENNUATION THRESHOLD

ATTENUATION THRESHOLD	$T = 5$ dB	$T = 10$ dB
CASE 1 : UNRELATED	52.9 %	40.3 %
CASE 2 : AOA DEPENDENCE	53.9 %	37.2 %
CASE 3 : RAY GROUPS	54.8 %	65.7 %

Once again, the choice of threshold has a greater effect on the mean values of the parameters, as oppose to the standard deviation. Also the parameter A_1 seems to be

less affected. The mean and standard deviation for the optimum and suboptimum cases are given in Table 7.

TABLE 6
EFFECT OF THRESHOLD ON THE MEAN VALUES AND STANDARD DEVIATIONS OF THE PARAMETERS OF THE COMPLEX POLYNOMIAL EXPANSION MODEL

ATTENUATION THRESHOLD		$T = 5$ dB		$T = 10$ dB	
PARAMETER		Mean Value	Standard Deviation	Mean Value	Standard Deviation
CASE 1 : UNRELATED	A_0	0.403	0.175	0.277	0.130
	A_1 (MHz^{-1})	0.148×10^{-3}	0.145×10^{-3}	0.150×10^{-3}	0.146×10^{-3}
	B_1 (MHz^{-1})	1.099×10^{-6}	0.220×10^{-3}	2.216×10^{-6}	0.249×10^{-3}
	$a_0 = 20\log A_0$	-8.98	4.90	-12.29	4.88
CASE 2 : AOA DEPENDENCE	A_0	0.364	0.146	0.2226	0.088
	A_1 (MHz^{-1})	0.051×10^{-3}	0.044×10^{-3}	0.050×10^{-3}	0.043×10^{-3}
	B_1 (MHz^{-1})	-0.077×10^{-6}	0.070×10^{-3}	-0.15×10^{-6}	0.074×10^{-3}
	$a_0 = 20\log A_0$	-9.81	4.87	-13.86	4.70
CASE 3 : RAY GROUPS	A_0	0.369	0.152	0.241	0.095
	A_1 (MHz^{-1})	0.091×10^{-3}	0.085×10^{-3}	0.088×10^{-3}	0.078×10^{-3}
	B_1 (MHz^{-1})	0.024×10^{-6}	0.110×10^{-3}	-0.57×10^{-6}	0.121×10^{-3}
	$a_0 = 20\log A_0$	-9.69	4.81	-13.32	4.58

TABLE 7
THE MEAN VALUES AND STANDARD DEVIATIONS OF THE PARAMETERS OF THE COMPLEX POLYNOMIAL EXPANSION MODEL FOR T = 10 DB

PARAMETER		OPTIMUM CASE $(A_2 = B_2 = 0)$		SUBOPTIMAL CASE $(A_2 = B_2 \neq 0)$	
		Mean Value	Standard Deviation	Mean Value	Standard Deviation
CASE 1	A_0	0.232	0.104	0.343	0.136
	A_1 (MHz^{-1})	0.181×10^{-3}	0.166×10^{-3}	0.105×10^{-3}	0.095×10^{-3}
	B_1 (MHz^{-1})	0.432×10^{-6}	0.024×10^{-3}	4.86×10^{-6}	0.263×10^{-3}
CASE 2	A_0	0.206	0.088	0.261	0.074
	A_1 (MHz^{-1})	0.063×10^{-3}	0.047×10^{-3}	0.028×10^{-3}	0.020×10^{-3}
	B_1 (MHz^{-1})	-0.102×10^{-6}	0.072×10^{-3}	-0.237×10^{-6}	0.078×10^{-3}
CASE 3	A_0	0.210	0.091	0.282	0.085
	A_1 (MHz^{-1})	0.108×10^{-3}	0.090×10^{-3}	0.061×10^{-3}	0.044×10^{-3}
	B_1 (MHz^{-1})	-0.659×10^{-6}	0.114×10^{-3}	-0.447×10^{-6}	0.128×10^{-3}

The histograms for these parameters are given in Figure 9. The shape of the distribution functions are again smooth and may be expressed as conventional statistical distributions. In the suboptimal cases, the values for A_2 and B_2 are of the order 10^{-20}. This justifies the assumption $A_2 = B_2 \approx 0$ and the subsequent usage of the truncated single order polynomial. The histograms of the parameters $A_2\left(\text{MHz}^{-2}\right)$ and $B_2\left(\text{MHz}^{-2}\right)$ for case 1 (unrelated parameters) are given in Figure 10.

The complex polynomial representation of the channel transfer functions is particularly advantageous when lower order polynomials are applicable. The model suggests the form of an adaptive equaliser response, $1/H_c(\omega)$, which is highly effective against multipath fading, when $A_1 > 0$. However, if $A_1 < 0$, the result is a

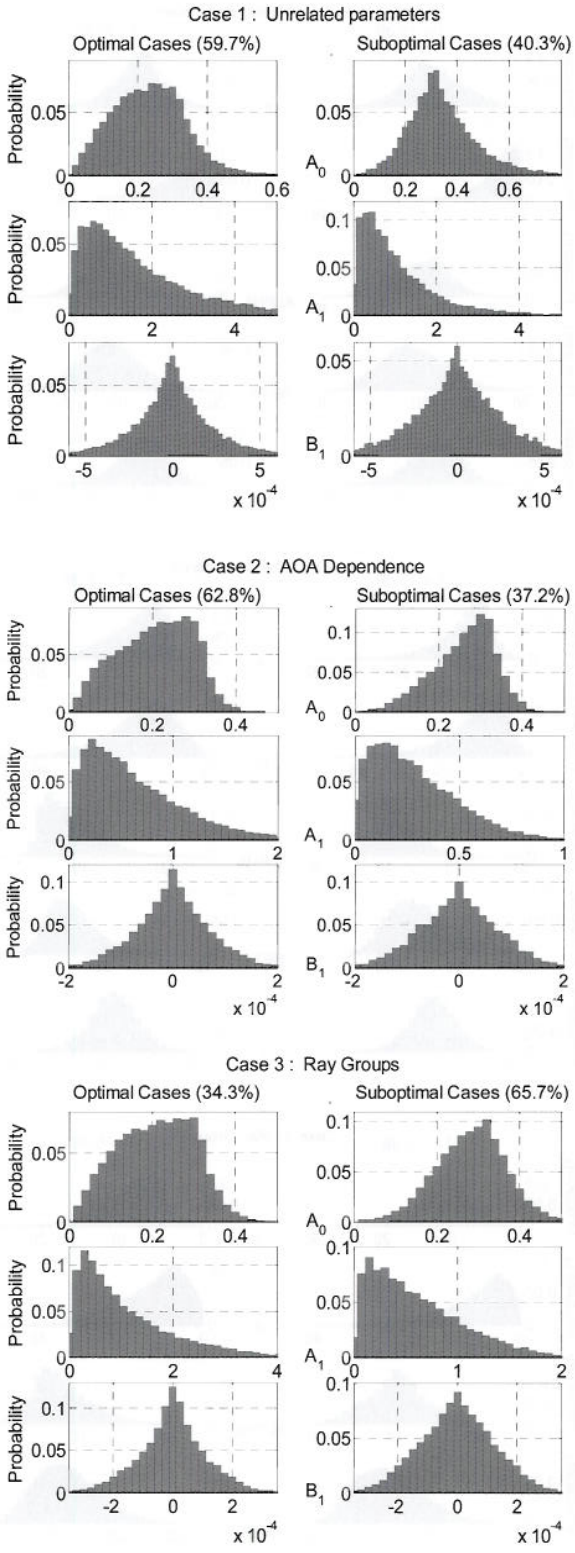

Figure 9: Histograms of the parameters of the polynomial model for optimal cases (left) and suboptimal cases (right), with $T = 10$ dB

reduction of the amplitude distortion at the expense of increased delay distortion. Future work will encompass the modelling of measured channel transfer functions from the LOS link, with the complex polynomial expansion method.

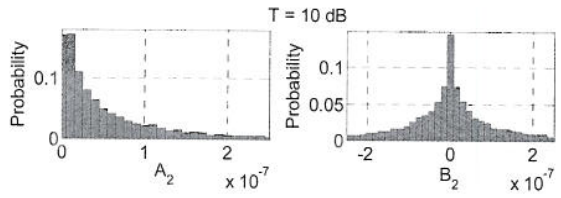

Figure 10: Histograms of the second order parameters, A_2 (MHz^{-2}) and B_2 (MHz^{-2}) for suboptimal cases, for case 1 with $T = 10$ dB.

8. CONCLUSION

Comprehensive channel models and channel measurements are of great value in system planning. Such knowledge and data provide an essential tool in optimizing channel usage. There exists tremendous potential for the use of millimetre-waves in terrestrial links, due to the better spectral availability and higher bandwidths that are possible. This exposes the need to perform accurate channel measurements and develop channel models at these frequencies. To achieve this goal, long term experiments need to be implemented hence a LOS link was established between the Howard College and Westville campuses of the University of KwaZulu-Natal (UKZN). However, such experiments are few and far between and to overcome this scarcity of available measurements, one can use computer generated channel transfer functions.

In this paper the simulation and statistical modelling of the above-mentioned LOS link is discussed. Three different simulation approaches were adopted to generate channel transfer functions.

For each approach, the channel transfers were modelled using the fixed delay two-ray model and the complex polynomial expansion method. The relevant parameters of the models were then statistically analysed. Future work will encompass the recording of the signal strength and delay spread of the link over a period of 1 year. These measurements will then be modelled as discussed in this paper. The resultant channel fading models can then be used to predict the outage time for the LOS link.

9. REFERENCES

[1] A.W. Straiton, "The Absorption and Reradiation of Radio Waves by Oxygen and Water Vapor in the Atmosphere", *IEEE Trans. on Antennas and Propagation*, vol. 23, no. 5, pp. 595-597, July 1975.

[2] R.K Crane, "Attenuation due to Rain", *IEEE Trans. on Antennas and Propagation*, vol. 23, no. 5, pp. 750-725, Sept. 1975.

[3] W. D. Rummler, "A New Selective Fading Model : Application to Propagation Data" *Bell System Technical Journal*, vol. 58, no. 5, pp. 1037–1071, May/ June 1979.

[4] L. J. Greenstein and B. A. Czekaj, "A New Selective Fading Model : Application to Propagation Data" *Bell System Technical Journal*, vol. 59, no. 7, pp. 1197–1225, September 1980.

[5] J. Lavergnat, M. Sylvain and J. Bic, "A Method to Predict Multipath Effects on a Line-of-Sight Link," *IEEE Trans. on Comm.*, vol. 38, no. 10, pp. 1810–1822, October 1990.

[6] L. J. Greenstein and M Shafi, *Microwave Digital Radio*. New York: IEEE Press, 1988.

[7] J. Lavergnat and P. Golé, "Statistical Behaviour of a simulated microwave multipath channel.," *IEEE Trans. on Antennas and Propagation*, Vol. 39, No. 12, pp. 1697–1706, December 1991.

[8] M. Sylvain and J. Lavergnat, "Modelling the transfer function in medium bandwidth radio channels during multipath propagation," *Ann. Télécummun.*, vol. 40, no. 11-12, pp. 584-603, 1985.

[9] ITU-R P.530-10; Propagation Data and Prediction Methods Required for the Design of Terrestrial Line-of-Sight Systems.

[10] K. Naicker and S.H. Mneney, "Propagation measurements and modeling for terrestrial line-of-sight links at 19.5 GHz," *in Proc. Africon'04, Gaborone, Botswana, September 15-17, 2004*

[11] K. Naicker and S.H. Mneney, "Multipath channel modeling for terrestrial line-of-sight links at 19.5 GHz.," *in Proc. SATNAC'04 Stellenbosch, South Africa, September 6-8, 2004.*